Available online at www.sciencedirect.com
ScienceDirect
International Journal of Heat and Mass Transfer 50 (2007) 2605–2611
International Journal of HEAT and MASS TRANSFER
www.elsevier.com/locate/ijhmt

Experimental study of forced convection heat transfer from a cam shaped tube in cross flows

A. Nouri-Borujerdi [a,*], A.M. Lavasani [b]

[a] School of Mechanical Engineering, Sharif University of Technology, Tehran, Iran
[b] Islamic Azad University, Science and Research Branch, Tehran, Iran

Received 31 August 2006; received in revised form 31 October 2006
Available online 2 February 2007

Abstract

An experimental investigation has been conducted to clarify forced convection heat transfer characteristic and flow behavior of an isothermal cam shaped tube in cross flow. The range of angle of attack and Reynolds number based on an equivalent circular tube are within $0° < \alpha < 180°$ and $1.5 \times 10^4 < Re_{eq} < 2.7 \times 10^4$, respectively.

The results show that the mean heat transfer coefficient is a maximum at about $\alpha = 90°$ over the whole range of the Reynolds numbers. It is found that thermal hydraulic performance of the cam shaped tube is larger than that of a circular tube with the same surface area except for $\alpha = 90°$ and 120°. Furthermore, the effect of the diameter of the cam shaped tube upon the thermal hydraulic performance is discussed.

Keywords: Experiment; Heat transfer; Cross flow; Cam shaped tube; Pressure drag

1. Introduction

Circular tubes are almost exclusively used in the construction of heat exchangers, primarily because of the ease of manufacture. In contrast to the circular tubes which cause severe separation and large wakes to produce high-pressure drops, non-circular tubes of streamlined shapes offer very low hydraulic resistance and consequently require less pumping power. In recent years, elliptic and oval tubes have been considered as heat transfer elements in cross flow heat exchangers.

Forced convection elliptic tubes was reported by Seban and Drake [1] and Drake et al. [2] who measured the local heat transfer coefficient for small angles of inclination ($0° < \alpha < 6°$). Kikkawa and Ohnishi [3] investigated unsteady combined forced and natural convection heat transfer from horizontal circular and elliptic tubes for $Re = 40$ and 80, respectively. They solved the two-dimensional Navier–Stokes and energy equations numerically and studied the thermal field experimentally in detail. Ota et al. [4,5] measured the heat transfer characteristic of airflow behavior for elliptic tubes with axis ratios of 1:2 and 1:3. In this work, the Reynolds number ranged from about 8000 to 79 000 with angle of attack from 0° to 90°. They found that the maximum mean heat transfer coefficient occurred within $60° < \alpha < 90°$ over the whole range of the Reynolds number. They also concluded that the minimum mean heat transfer rate for an elliptic tube was higher than that for a circular tube. Studies of Ota et al. [6] also illustrate that the local heat transfer coefficient around two elliptic tubes with an axis ratio of 1:2 placed in tandem in cross flow depends strongly upon the angle of attack and tubes spacing.

Merker and Hanke [7] reported heat transfer and pressure drop on the shell-side of oval-shaped tubes bank. Their results show that exchangers with oval-shaped tubes have considerably smaller frontal areas on the shell-side compared to those with circular tubes.

* Corresponding author.
E-mail addresses: anouri@sharif.edu (A. Nouri-Borujerdi), a_lavasani@iauctb.ac.ir (A.M. Lavasani).

0017-9310/$ - see front matter © 2006 Published by Elsevier Ltd.
doi:10.1016/j.ijheatmasstransfer.2006.11.028

Nomenclature

C_p	specific heat, static pressure coefficient
C_D	pressure drag coefficient
D	large diameter
d	small diameter
Gr	Grashof number, $g\beta\Delta TD^3/v\alpha^2$
h	heat transfer coefficient
k	thermal conductivity
L	tube length
l	distance between centers
$\dot{m}$	mass flow rate
Nu	Nusselt number, hD/k
P	circumferential length of the cam, pressure
$\dot{Q}$	heat transfer rate
$\dot{q}''$	heat flux rate
Ra	Rayleigh number, $g\beta\Delta TD^3/\alpha v$
Re	Reynolds number, $U_\infty D/\upsilon$
S	distance from leading edge
St	Stanton number, $h/\rho C_P U_\infty$
T	temperature
U	velocity
$\dot{V}$	volume flow rate
y	y-coordinate

Greek symbols

α	angle of attack, thermal diffusivity
β	expansion coefficient, angle
Δ	difference
v	kinematic viscosity
ρ	density
ψ	angle of hole

Superscript

-	mean

Subscripts

a	air
eq	equivalent
f	film
i	inlet
o	outlet
s	surface
∞	free stream
w	water

Ilgarubis and Butkus [8] reported forced convection from elliptical finned tubes. They investigated experimentally the heat transfer characteristics for the Reynolds numbers up to 4×10^3.

Prasad et al. [9] reported heat transfer and pressure drop from an airfoil in cross flow. The airfoil test section was the NACA-0024 and they concluded that this shape gives higher values of Stanton number to pressure loss coefficient compared to a circular tube.

Badr and Shamsher [10] and Badr [11] carried out numerical studies on free convection from isothermal horizontal elliptic tubes. Both works were based on the solution of full conservation equations of mass, momentum, and energy with no boundary-layer simplifications. Badr and Shamsher solved the problem of free convection from an elliptic tube for the Rayleigh numbers ranging $10 < Ra < 10^3$, and axis ratios ranging from 0.1 to 0.964.

Rocha et al. [12] compared elliptic and circular tubes in specific cases of one and two-row tube with plate fin heat exchangers. The results illustrate that heat transfer gain is achieved up to 18% when using elliptic tubes instead of circular tubes arrangement.

Badr [13] reported forced convection heat transfer from an isothermal elliptic tube in cross flow. In this study, the range of Reynolds number and inclination are $20 < Re < 500$ and $0° < \alpha < 90°$ respectively. The tube axes ratio varies from 0.4 to 0.9. The results show that the maximum rate of heat transfer reaches at $\alpha = 0°$ while the minimum occurs at $\alpha = 90°$.

Bordalo and Saboya [14] conducted pressure drop measurements for elliptic and circular tubes as well as a plate fin heat exchanger with one, two and three-row arrangement. They reported that with the elliptic configuration, the reduction of pressure drop coefficient could be achieved up to 30% due only to the presence of the tubes.

Castiglia et al. [15] studied in detail the flow over an in-line array of elliptic tubes in cross flow with an axes ratio of 1:2. They showed that this configuration generates significantly lower turbulence levels than an equivalent array with circular tubes.

Badr et al. [16] predicted form drag and skin friction of an oval tube at various orientations with the major axis parallel to the flow direction. The total drag coefficient is 0.9 at $Re = 700$ and 0.8 at $Re = 3700$ for an oval with a length ratio of minor-to-major axis equal to 0.6. The form drag is 80–90% of the total drag. The drag force decreases as the oval tube is made more slender, i.e., the shape factor is decreased. Compared with a circular tube, the drag coefficient is reduced between 10% and 20%.

Hasan and Siren [17] carried out experiments to compare the performance of a plain circular and an oval tube in evaporative cooling heat exchangers. They concluded that the ratio of average mass transfer Colburn factor to average friction factor for oval tubes is 1.93–1.96 times that for circular tubes. This means that the oval tubes have a better-combined thermal hydraulic performance.

Tiwari et al. [18] reported a three-dimensional computational study of forced convection heat transfer to determine the flow structure and heat transfer in a rectangular chan-

nel with a built-in oval tube and delta wing type vortex generators in various configurations. Their results indicate that vortex generators in conjunction with the oval tubes show definite promise for the improvement of fin–tube heat exchangers.

Matos et al. [19] studied the heat transfer rate numerically and experimentally for a staggered arrangement of circular and elliptic finned tubes in an external flow. They have reported that the optimal elliptic arrangement exhibits a heat transfer gain up to 19% compared to the optimal circular tube arrangement. The results illustrate that the heat transfer gain and the relative total mass reduction up to 32% show that the elliptical arrangement has the potential to deliver considerably higher global performance and lower cost.

Bouris et al. [20] carried out experimental and numerical simulation on the novel tubes bank heat exchanger to study the thermal, hydraulic and fouling characteristics. The proposed tube cross section was termed deposit determined fouling reducing morphology tube. Their results indicate that they attain higher heat transfer levels with 75% lower deposition rate and 40% lower pressure drop.

It is well established that a cam shaped tube has a low value of drag coefficient; however, not much work has been reported on its heat transfer capability especially under an angle of attack. The purpose of this study is to investigate the mean heat transfer coefficient of a cam shaped tube.

2. Experimental apparatus

A schematic diagram of an experimental apparatus is shown in Fig. 1. The test rig consists of an open wind tunnel with a circular duct and diameter of 0.24 m. The test section with dimension 20 × 32 × 20 cm is located at a distance of 10 cm in front of the tunnel outlet and designed to measure the rate of heat transfer and drag force of a single

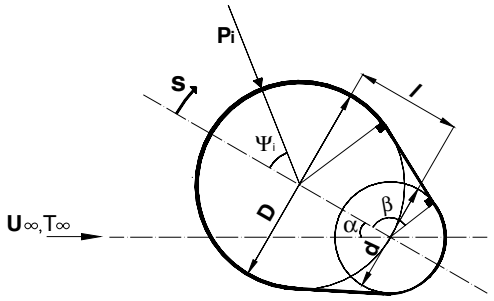

Fig. 2. Schematic diagram of a cam shaped tube cross section.

cam shaped tube in cross flow. The tube is mounted horizontally between the test section walls such that it is perpendicular to flow direction. The cross section of the cam shaped tube consists of two circles with different diameters (d, D) and a distance l between their centers (Fig. 2). In the figure, $0° \leqslant \alpha \leqslant 180°$ denotes the inclination angle between the major axis of the cam shaped tube with the direction of upstream flow. The tube is made of commercial copper plate with 0.3 mm thickness.

A variable speed motor (in Fig. 1) is used to generate a uniform free stream in front of the test section with velocity in the range of 12–22 m/s. Fig. 3 depicts the velocity profiles and their mean values across flow field with 5% uncertainty.

To heat up the tube, a pump circulates hot water between a tank and the tube. An electric heating element supplies the hot water and a control valve regulates the hot water at the tube inlet. Water temperature is measured at the inlet and outlet of the tube using type-k thermocouple wires. A glass tube flow meter measures the flow rate with 1% uncertainty in full-scale flow. A steady state condition is reached between 10 and 30 min, depending on the ambient temperature and free stream velocity, and then data collection is started.

In order to make more clear correlations between the heat transfer and flow characteristics, another cam shaped

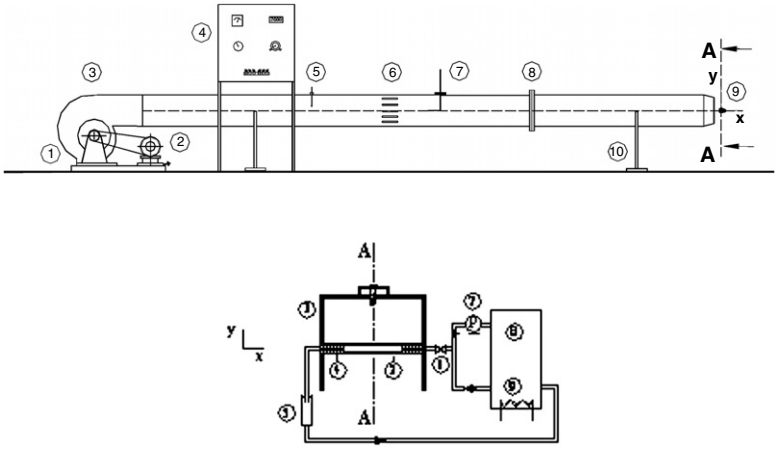

1-Variable speed mechanism 2-Driving Motor 3-Centrifugal Blower 4-Control panel 5-Thermometer
6-Honeycombs 7-pitot tube 8-Orifice 9-Test section 10-Supporter
11-Flow meter 12-Control valve 13-Supporterframe 14-Insulation 15-Pump
16-Heating element 17-Tank

Fig. 1. Schematic diagram of the experimental test rig.

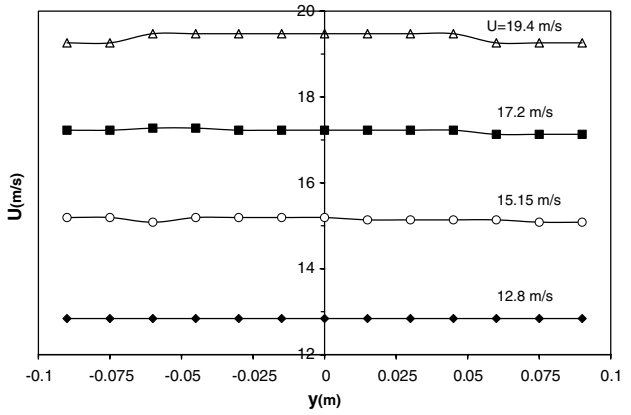

Fig. 3. Distribution of free stream velocity in the front of the test section.

tube is also used to measure static pressure around the tube. This tube is almost the same as the one used before for heat transfer study. Its surface is covered with 20 holes (1 mm in diameter) drilled to measure the static pressure on the tube surface by a dial manometer.

3. Experimental technique and measurement uncertainties

To investigate the effect of cam shaped tube dimensions on heat transfer, three tubes with different sizes are tested. The dimensions of each tube are given in Table 1. D_{eq} is the diameter of an equivalent circular tube whose circumferential length is equal to that of the cam shaped tube. Based on Fig. 2, the equivalent diameter, D_{eq}, is obtained by

$$D_{eq} = \frac{P}{\pi} = \frac{1}{2}\left(1+\frac{d}{D}\right) + \frac{1}{\pi}\left(1-\frac{d}{D}\right)\left[\sin^{-1}\left(\frac{D-d}{2l}\right) + \sqrt{\left(\frac{D-d}{2l}\right)^2 - 1}\right] \quad (1)$$

where p is the circumferential length of the cam shaped tube.

To avoid end effects, the tube length L is extended 10 cm from each side with insulation materials and without any change in cross section area. The tube with $L/D_{eq} > 4$ has little end effect on heat transfer. For $1.5 \times 10^4 < Re_{eq} < 2.7 \times 10^4$, this effect on heat transfer rate from the second and third tube with $L/D_{eq} = 3.36$ and 2.03 is 4–6% and 6–10% respectively [21]. The rate of heat transfer from the tube to the air is obtained by measuring mass flow rate, inlet and outlet water temperatures through the tube as

$$\dot{Q}_w = \dot{m}_w C_{p,w}(T_{wi} - T_{wo}) \quad (2)$$

where $\dot{m}_w = \rho_w \dot{V}_w \cdot C_{p,w}$, ρ_w and $\dot{V}_w$ are specific heat, density and volume flow rate of water respectively.

Based on the minimum value of the free stream velocity (i.e., 12 m/s), the maximum value of Gr_{eq}/Re_{eq}^2 for a cam shaped tube with $D_{eq} = 24.7$ mm is about 1.29×10^{-4}. The heat loss radiation from the tube surface is estimated to be about 1–1.5% of heat supplied. Hence, the effect of natural convection and radiation can be neglected in the calculations.

The mean Nusselt number is determined as follows:

$$\overline{Nu}_{eq} = \frac{\bar{h}D_{eq}}{k} = \frac{\dot{Q}_w}{\pi L k (T_S - T_\infty)} \quad (3)$$

where k is the thermal conductivity of air evaluated at film temperature. T_∞ and T_S represent respectively the ambient and mean tube surface temperature.

The pressure drag coefficient C_D is determined experimentally from pressure distribution over the cam shaped tube surface, including the large and small circles as well as two tangent lines between them as follows:

$$C_D = \frac{1}{D_{eq}}\oint C_P \cos\psi \mathrm{d}s = \frac{1}{D_{eq}}\left\{\sum_{i=1}^{20} C_{p,i}[m\cos(\alpha+\psi_i) - (1-m)\cos(\alpha+\beta)]\Delta S_i\right\} \quad (4)$$

$$C_p = \frac{P - P_\infty}{\frac{1}{2}\rho U^2} \quad (5)$$

α is angle of attack, ψ_i is angle between line of axi-symmetry and radius through hole i on either large or small circle. β is a constant and its values for cam shaped tubes 1–3 according to Table 1 are 117.03°, 99.92°, and 94.34° respectively. ΔS_i represents a length on the tube perimeter belong to each hole. Value of m for holes on the circles and line of tangent are 1 and 0 respectively.

The accuracy of the mean Nusselt number can easily be obtained by differentiation of Eq. (3) after substitution Eq. (2) into Eq. (3) as follows:

$$\Delta(\overline{Nu}_{eq}) = \overline{Nu}_{eq}\left[\left|\frac{\Delta(\dot{m}_w)}{\dot{m}_w}\right| + \left|\frac{\Delta(T_{wi})}{T_{wi}-T_{wo}}\right| + \left|\frac{\Delta(T_{wo})}{T_{wi}-T_{wo}}\right| + \left|\frac{\Delta(T_s)}{T_s - T_\infty}\right| + \left|\frac{\Delta(T_\infty)}{T_s - T_\infty}\right| + \left|\frac{\Delta(k)}{k}\right| + \left|\frac{\Delta(C_{p,w})}{C_{p,w}}\right| + \left|\frac{\Delta(L)}{L}\right|\right] \quad (6)$$

Table 1
Dimensions of test cam shaped tubes

Tube no.	d (mm)	l (mm)	D (mm)	$D_{eq} = P/\pi$ (mm)	L (mm)	L/D_{eq}	l/D
1	12	11	22	$24.7 = 77.7/\pi$	120	4.85	0.5
2	12	29	22	$35.7 = 112.2/\pi$	120	3.36	1.3
3	12	66	22	$59.1 = 185.7/\pi$	120	2.03	3

where $\Delta(T_{wi})$ and $\Delta(T_{wo})$ are respectively, the measurement errors of the water inlet and outlet temperatures. $\Delta(T_s)$ and $\Delta(T_\infty)$ are similar errors for the mean surface and ambient temperatures respectively, each having a values of about ± 0.11 °C. The values of $\Delta(T_{wi})/(T_{wi} - T_{wo}) = \Delta(T_{wo})/(T_{wi} - T_{wo})$ and $\Delta(T_s)/(T_s - T_\infty) = \Delta(T_\infty)/(T_s - T_\infty)$ are respectively about ± 0.015 and ± 0.0075. The error in the mass flow rate can be obtained through $\Delta(\dot{m}_w) = \dot{m}_w\left[|\Delta(\rho_w)/\rho_w| + \left|\Delta\dot{V}/\dot{V}\right|\right]$, where $\Delta(\rho_w)$ and $\Delta(\dot{V})$ are the errors of the water density and volume flow rate. Since the errors of the flow meter is about $\pm 1 \times 10^{-8}$ m^3/s and that of the volume flow rate is about 1×10^{-6} m^3/s, the value of $\Delta(\dot{V})/\dot{V} = \pm 0.01$. The specific heat and density of water and the air thermal conductivity are functions of the water temperature and air film temperature. These functions can be obtained from the air and water physical properties [22]. These errors can be estimated as $\Delta(C_{p,w}) = |dC_{p,w}/dT_{f,w}|\Delta(T_{f,w})$, $\Delta(\rho_w) = |d\rho_w/dT_{f,w}|\Delta(T_{f,w})$ and $\Delta(k) = |dk/dT_{f,a}|\Delta(T_{f,a})$. Using the tables of thermodynamic properties of air and water, the mean specific heat, density and thermal conductivity gradients can easily be obtained in the range of the temperature variations. These values are ± 0.3, ± 0.09 and $\pm 0.8 \times 10^{-4}$. $\Delta(L)$ is measurement error of tube length with value of about ± 0.0005 m, making that $\Delta(L)/L$ to be about ± 0.004. Substituting the above-mentioned errors in Eq. (5), the mean Nusselt number uncertainty is about ± 4.5–5.5%.

4. Results and discussion

A single circular tube with diameter 2.47 cm and length 15 cm is tested before testing the cam shaped tube, to verify the data-taking process and to check the related equipment setup. Experiments are carried out with nominal tube surface temperature of about 75 °C and air temperature about 25 °C. Fig. 4 compares the present results with the results of Zhukauskas [23]. There is a difference of about 1–5% between the present results and the results of Zhukauskas. The friction coefficient of the circular tube is measured and it is 0.76–0.79 in the range of $1.6 \times 10^4 < Re < 2.7 \times 10^4$. The difference between the present results and that of curve-fit formula by White [24] is about 1–4%.

Fig. 5 represents the pressure distributions along the cam shaped-tube surface for different angles of attack. The x-axis indicates distance from the leading edge of the tube; positive values indicate the distance along the upper surface and negative ones indicate the distance along the lower surface as shown in Fig. 2. When the cam tube rotates in the clockwise direction, the stagnation point moves on the lower. It can be detected that at $\alpha = 90°$, the upstream separation point almost coincides with the leading edge. A large wake downstream of the tube may bring about a violent motion of fluid therein and it results in a high heat transfer rate as demonstrated previously.

Variation of C_D with α is shown in Fig. 6. The drag coefficient decreases with angle of attack until $\alpha = 30°$. After that it increases until $\alpha = 90°$ and decreases until $\alpha = 180°$. It is to be noted that the present value of C_D is based upon the equivalent diameter as the reference length scale.

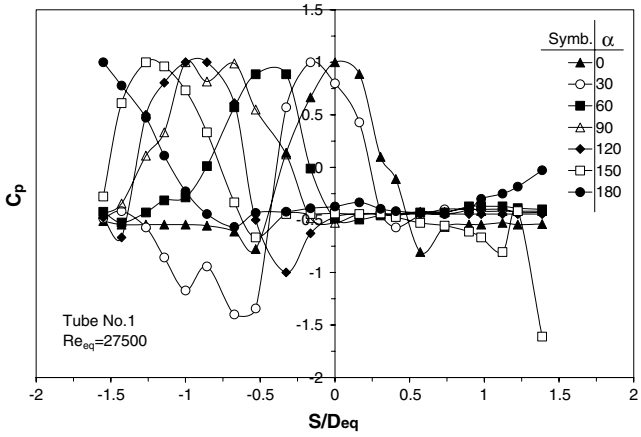

Fig. 5. Pressure coefficient along surface of the cam shaped tube for different angles of attacks.

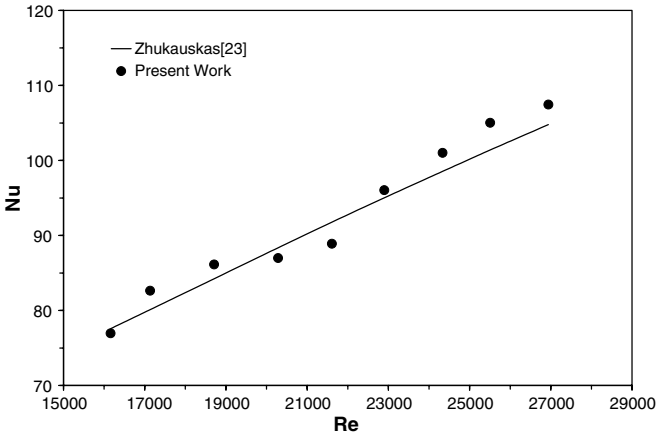

Fig. 4. Mean Nusselt number of a circular tube in a cross flow.

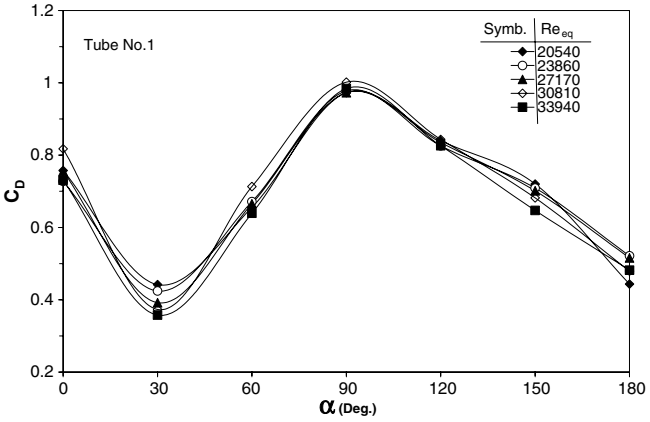

Fig. 6. Pressure drag coefficient vs. angle of attack for different Reynolds numbers.

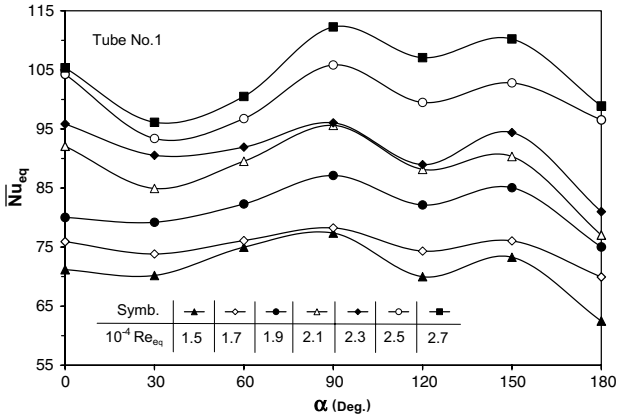

Fig. 7. Mean Nusselt number of cam shaped tube vs. angle of attack for different Reynolds numbers.

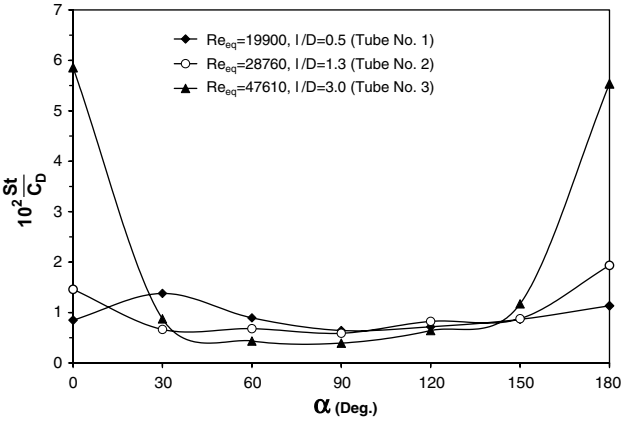

Fig. 9. Stanton number to drag coefficient ratio vs. angle of attack for different l/D.

Fig. 7 indicates that the mean Nusselt number does not increase monotonically with α. As α increases from zero, $\overline{Nu}_{eq}$ first decreases and reaches a minimum value at around $\alpha = 30°$. Then it increases and attains a maximum value over the whole Reynolds number range studied at about $\alpha = 90°$. Subsequently it decreases once again around $\alpha = 120°$. In the region of $\alpha = 30°$, the decrease of the oncoming flow velocity to the upstream surface of the tube brings about a relatively low value of $\overline{Nu}_{eq}$. Furthermore, in the separated flow region, the heat transfer rate is not so high since the transversal motion of fluid may not be so severe as in the case of $\alpha > 30°$. These facts may result the minimum value of $\overline{Nu}_{eq}$ observed at $\alpha = 30°$.

Comparison between thermal hydraulic performance of a cam shaped tube with $d/D = 0.54$ and $l/D = 0.5$ for $\alpha = 0°$–$180°$ and one circular tube having the same circumferential length ($D = 24.7$ mm) is shown in Fig. 8. Thermal hydraulic performance of the cam shaped tube for any angles of attack is nearly constant and does not change too much with Reynolds number. This figure illustrates that St/C_D is maximum at $\alpha = 30°$ and also is higher than that of the circular tube. The maximum value is corresponding to the minimum value of drag coefficient at

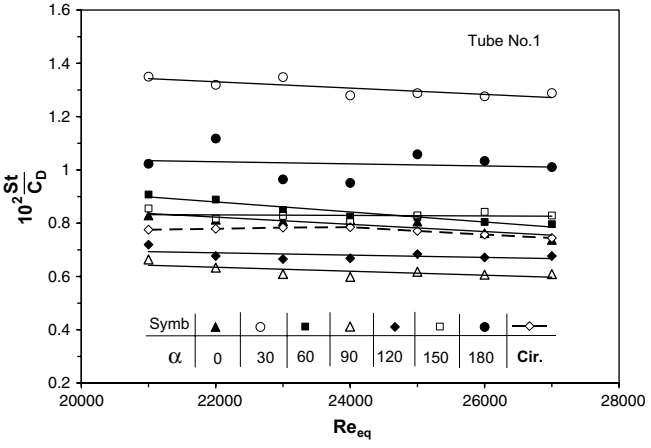

Fig. 8. Comparison of Stanton number to drag coefficient ratio for circular and cam shaped tube with the same circumferential length.

$\alpha = 30°$ as shown in Fig. 6. The difference between the maximum ($\alpha = 30°$) and minimum $\alpha = 90°$ values of the thermal hydraulic performance is about 52%. The figure also includes St/C_D of a circular tube shown by dot line. Its value is higher than that of the cam shaped tube at $\alpha = 90°$, and 120°.

The effect of l/D ratio on St/C_D for three tubes is reported in Fig. 9 for the same $d/D = 0.54$ and $U = 15$ m/s. The value of l/D for each tube is given in Table 1. St/C_D for three tubes is quite constant and nearly the same in the range of $30° < \alpha < 150°$. Out side this range, the variation is significant and strongly depends on Reynolds number. The main reason is due to the low value of the tube drag coefficient at high l/D. The value of St/C_D for $l/D = 3$ at $\alpha = 0°$, 180° is very high compared with the other tubes.

5. Conclusions

The mean heat transfer characteristics and pressure distribution of an isothermal cam shaped tube were investigated experimentally. The angle of attack is varied in the range of $0° < \alpha < 180°$ over the $1.5 \times 10^4 < Re_{eq} < 2.7 \times 10^4$.

The dependency of the mean Nusselt number on the angle of attack and Reynolds number is quite clear from the results. These Results show that the heat transfer from a cam shaped tube is a maximum value at about $\alpha = 90°$ and is a minimum at $\alpha = 30°$. The effects of the l/D for the cam shaped tube with the same d/D upon its thermal hydraulic performance are also investigated. These results indicate that for large l/D the performance is a maximum at $\alpha = 0°$ and 180°, but is a minimum at $\alpha = 90°$.

In order to compare the available Stanton number and pressure drag of the cam shaped tube with that of a circular tube with the same circumferential length, a Reynolds number based on an equivalent diameter has been defined. These comparisons have shown that cam shaped-bodies give larger values of St/C_D except at $\alpha = 90°$ and 120° relative to the circular tubes.

References

[1] R. Seban, R. Drake, Local heat-transfer coefficients on the surface of an elliptic cylinder in a high speed air stream, Trans. ASME 75 (1953) 235–240.

[2] R. Drake, R. Seban, D. Doughty, S. Lin, Local heat transfer coefficients on the surface of an elliptic cylinder, axis ratio 1:3, in a high speed air stream, Trans. ASME 75 (1953) 1291–1302.

[3] S. Kikkawa, T. Ohnishi, Unsteady combined forced and natural convective heat transfer from horizontal circular and elliptic cylinder, Sci. Eng. Rev. Doshisha Univ. 19 (2) (1974).

[4] T. Ota, S. Aiba, T. Tsuruta, M. Kaga, Forced convection heat transfer from an elliptic cylinder of axis ratio 1:2, Bull. JSME 26 (1983) 262–267.

[5] T. Ota, H. Nishiyama, Y. Taoka, Heat transfer and flow around an elliptic cylinder, Int. J. Heat Mass Transfer 27 (1984) 1771–1779.

[6] T. Ota, H. Nishiyama, J. Kominami, K. Sato, Heat transfer from two elliptic cylinders in a tandem arrangement, J. Heat Transfer 18 (1986) 525–531.

[7] G.P. Merker, H. Hanke, Heat transfer and pressure drop on the shell-side of tube-banks having oval-shaped tubes, Int. J. Heat Mass Transfer 29 (12) (1986) 1903–1909.

[8] R. Ilgarubis Ulinskas, A. Butkus, Hydraulic drag and average heat transfer coefficients of compact bundles of elliptical finned tubes, Heat Transfer-Soviet Res. 20 (1) (1988) 12–21.

[9] B.V.S.S.S. Prasad, A.A. Tawfek, V.R.M. Rao, Heat transfer from aerofoils in cross-flow, Int. Commun. Heat Mass Transfer 19 (1992) 870–890.

[10] H.M. Badr, K. Shamsher, Free convection from an elliptic cylinder with major axis vertical, Int. J. Heat Mass Transfer 36 (1993) 3593–3602.

[11] H.M. Badr, Laminar natural convection from an elliptic tube with different orientations, ASME J. Heat Transfer 119 (1997) 709–718.

[12] L.A.O. Rocha, F.E.M. Saboya, J.V.C. Vargas, A comparative study of elliptic and circular sections in one and two-row tubes and plate fin heat exchangers, Int. J. Heat Fluid Flow 18 (1997) 245–252.

[13] H.M. Badr, Force convection from a straight elliptical tube, Int. J. Heat Mass Transfer 34 (1998) 229–236.

[14] S.N. Bordalo, F.E.M. Saboya, Pressure drop coefficients for elliptic and circular sections in one, two and three-row arrangements of plate fin and tube heat exchangers, J. Braz. Soc. Mech. Sci. XXI 4 (1999) 600–610.

[15] D. Castiglia, S. Balabani, G. Papadakis, M. Yianneskis, An experimental and numerical study of the flow past elliptic cylinder arrays, Proc. Inst. Mech. Engs. (ImechE) Part C 215 (2001) 1287–1301.

[16] H.M. Badr, S.C.R. Dennis, S. Kocabiyik, Numerical simulation of the unsteady flow over an elliptic cylinder at different orientations, Int. J. Numer. Meth. Fluids 37 (2001) 905–931.

[17] A. Hasan, K. Siren, Performance investigation of plain circular and oval tube evaporatively cooled heat exchangers, Appl. Therm. Eng. 24 (2003) 777–790.

[18] S. Tiwari, D. Maurya, G. Biswas, V. Eswaran, Heat transfer enhancement in cross-flow heat exchangers using oval tubes and multiple delta winglets, Int. J. Heat Mass Transfer 46 (2003) 2841–2856.

[19] R.S. Matos, T.A. Laursen, J.V.C. Vargas, A. Bejan, Three-dimensional optimization of staggered finned circular and elliptic tubes in forced convection, Int. J. Therm. Sci. 43 (2004) 477–487.

[20] D. Bouris, E. Konstantinidis, S. Balabani, D. Castiglia, G. Bergeles, Design of a novel, intensified heat exchanger for reduced fouling rates, Int. J. Heat Mass Transfer 48 (2005) 3817–3832.

[21] A. Quarmby, A.A.M. AL-Fakhri, Effect of finite length on forced convection heat transfer from cylinder, Int. J. Heat Mass transfer 23 (1980) 463–469.

[22] M. Netcati Ozisik, Heat Transfer, McGraw-Hill, New York, 1985.

[23] A. Zhukauskas, Heat Transfer of a Cylinder in Cross Flow, Hemisphere Publishing Corporation, 1985.

[24] F.M. White, Fluid Mechanics, McGraw-Hill, New York, 2005.